

A MATHEMATICAL MODEL OF THE BACTERIAL GENE NETWORK PARTIALLY RESPONSIBLE FOR REGULATING NITROGEN ASSIMILATION

Brian A. Blaugrund

April 4, 2005

Abstract

The regulation of nitrogen assimilation in various bacteria utilizes similar versions of a gene network characterized by negative and positive feedback signals on the *glnALG* operon. I developed a model that describes the dynamics of auxiliary ammonia levels, inhibitor protein concentration, and inducer protein concentration as factors in glutamine synthetase transcription. This model accounts for phosphorylation, coupled enhancer-binding, and constitutive feedback in the regulatory pathways. It was hypothesized that the glutamine synthetase concentration as a function of the ammonia concentration would contain a sharp nutrient supply threshold created by a multistable middle region. This region was expected to split oscillatory upper and lower regions denoting ammonia saturation and deprivation, respectively. The quasi steady state assumption for the ammonia resource depletion rate behaved visually identical to the non simplified form of the model. Furthermore, the validity of a rapidly equilibrating ammonia concentration for a very large initial ammonia supply supported ammonia as a favored nitrogen source.

Short Title: Gene network model

Key Words: Feedback, gene network, ammonia, glutamine synthetase, operon, transcription, quasi steady state

1 Introduction

The dynamic profile of intracellular protein and mRNA concentration has been described mathematically for a variety of gene networks. Autoregulation, which refers to the interaction between a gene's promoter and a product of that gene, has also been mathematically described. Positive autoregulation has been characterized as less stable and responsive relative to classical—or constitutive—operon regulation [1]. Negative autoregulation has been shown to exhibit high stability and low rise-time relative to non-constitutive operons [2]. Interestingly, both positive and negative autoregulation often act simultaneously, producing networks with more complicated patterns of gene regulation [3]. Dimerization, phosphorylation, contradicting autoregulatory feedback, or time delay in genetic regulatory systems contributes to transcriptional oscillations and multistability [4].

The regulation of nitrogen assimilation in *E. coli* contains each of these complexities [5]. I have constructed a mathematical model of a simplified network that describes the expression of genes in the *glnALG* operon. The purpose of this model is to predict whether complex behavior is expected in the nitrogen metabolism of *E. coli*. The model includes regulatory influence from the available ammonia supply. I hypothesize that a sharp nutrient supply threshold will divide oscillatory upper and lower regions denoting ammonia saturation and deprivation, respectively, with a multistable middle region. This threshold is predicted to exist around 1 mM based on other empirical experiments [6].

2 Biological Background

Glutamine and glutamate collectively provide all the nitrogen used by enteric bacteria for anabolism. Nitrogen is derived primarily from the amino functional group of glutamate but also arises to a lesser degree from the amide group in

glutamine. A large ammonia concentration allows direct production of glutamate from α -ketoglutarate, NADPH, and NH_3 in a pathway catalyzed by glutamate dehydrogenase.

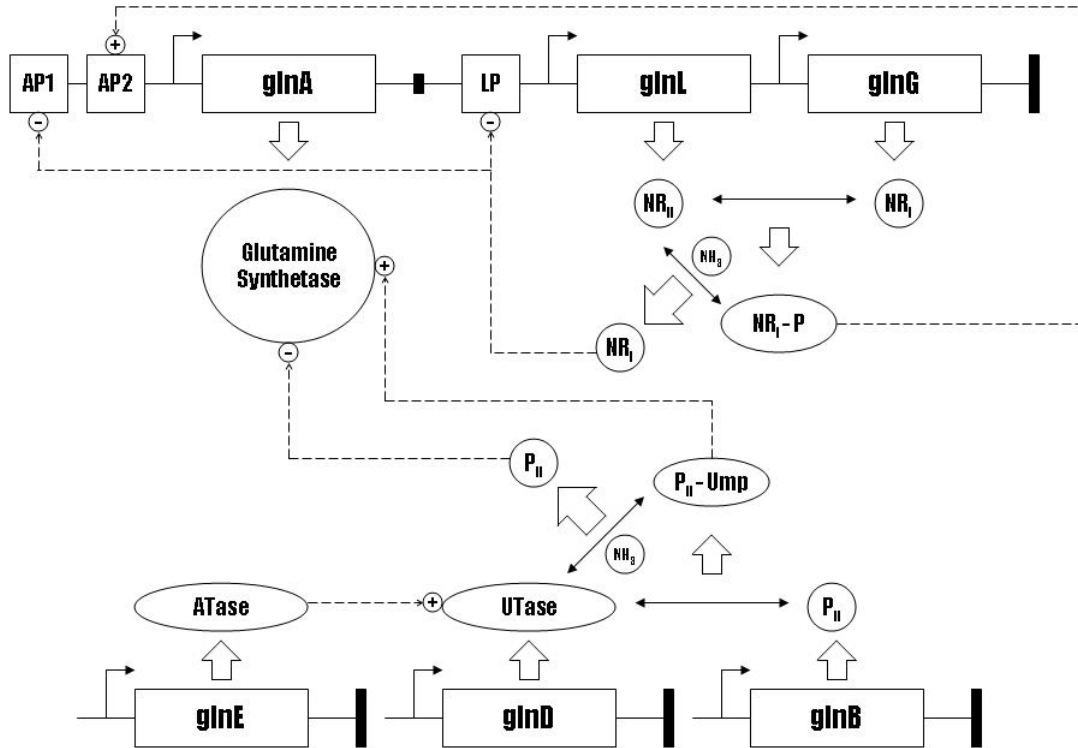


Figure 1 The collection of bacterial genes that play a role in the transcriptional regulation of glutamine synthetase. Solid lines are the open reading frame boundaries. Dashed lines show potential regulator activity. Block arrows represent the formation of a product. Solid arrows indicate the reactants of a respective synthesis reaction.

In an ammonia-deprived resource pool, a two step pathway yields glutamate, ADP, NADP^+ , and phosphate [7]. The first of these two steps is catalyzed by glutamine synthetase, which is the product of the *glnA* structural gene located near the start of the *glnALG* operon (Figure 1). The transcriptional product of *glnL* is the first regulator protein, NR_I . The transcriptional product of *glnG* is the second regulator protein, NR_{II} , which is responsible for phosphorylating NR_I into $\text{NR}_I\text{-P}$ under reduced-ammonia conditions and dephosphorylating $\text{NR}_I\text{-P}$ into NR_I under elevated-ammonia conditions [8]. Just

upstream of *glnA* are two separate promoter regions, *glnAp1* and *glnAp2*, which bind NR_I and NR_P , respectively. NR_I inhibits *glnA* expression when bound to *Ap1* and NR_P activates *glnA* expression when bound to *Ap2* [9]. Two molecules of NR_P must dimerize, bind to *Ap2*, and then interact with the transcription complex for this activation to occur [10].

Several other relevant unlinked structural genes include *glnB*, which codes for the protein P_{II} , *glnD*, which codes for uridylyltransferase (UTase), and *glnE*, which codes for adenylyltransferase (ATase). P_{II} stimulates the dephosphorylation of NR_I by NR_{II} (not shown in Figure 1), as well as the adenylation of glutamine synthetase by ATase. Buildup of this inactive form of glutamine synthetase is caused by an adequate ammonia concentration. In addition, Utase/UR uridylylates P_{II} into P_{II-U} when ammonia levels drop and deuridylylates P_{II-U} back into P_{II} when ammonia levels rise [5].

3 Mathematical Model

Let $G(t)$ be the concentration of glutamine synthetase in a single *E. coli* cell at time t . Let $N_I(t)$ be the concentration of NR_I , the product of *glnG*, in the cell. Let $N_{II}(t)$ be the concentration of NR_{II} , the product of *glnL*, in the cell. Also, let $N_3(t)$ be the concentration of phosphorylated NR_I in the nucleus. Finally, let $N_4(t)$ be the ammonia concentration available to the cell. The resulting model of the *gln* gene network takes the following form:

$$\begin{aligned}
\frac{dG}{dt} &= \frac{\alpha_1 N_3^2}{\lambda + \kappa_1 N_1 + N_3^2} + v_2 G \left(1 - \frac{N_4}{\varepsilon}\right) - \delta G - \frac{v_1 G N_4}{\varepsilon}, \\
\frac{dN_1}{dt} &= \frac{\kappa_2 \alpha_2}{\kappa_2 + N_1} + \frac{\beta_1 N_2 N_3 N_4}{\varepsilon} - \delta N_1 - \beta_2 N_1 N_2 \left(1 - \frac{N_4}{\varepsilon}\right), \\
\frac{dN_2}{dt} &= \frac{\kappa_2 \alpha_2}{\kappa_2 + N_1} - \delta N_2, \\
\frac{dN_3}{dt} &= \beta_2 N_1 N_2 \left(1 - \frac{N_4}{\varepsilon}\right) - \frac{\beta_1 N_2 N_3 N_4}{\varepsilon} - \delta N_3, \\
\frac{dN_4}{dt} &= \phi \left(1 - \frac{N_4}{\varepsilon}\right) - \frac{\mu G N_4}{\varepsilon} - \frac{\psi N_4}{\varepsilon}.
\end{aligned} \tag{1}$$

The definitions and units of the parameters are listed in Table 1. The two positive terms on the right-hand side of the dynamical glutamine synthetase equation describe the various routes of enzyme production. The first term accounts for simultaneous positive and negative autoregulation. When no repressor is present in the form of the unphosphorylated first regulator, then a dimer of the phosphorylated form induces glutamine synthetase production. The dimerization is represented by the squared variable. The second term describes the chemical activation of glutamine synthetase by ATase, which is influenced by the presence of ammonia. The interaction between a glutamine synthetase molecule and an ATase molecule is modeled through mass action, where the ATase multiplicand is replaced by an ammonia modifier scaled inversely between zero and one. It is assumed that the ammonia concentration adequately represents the complicated enzyme activation pathway involving ATase and UTase. The two negative terms in this equation represent removal of glutamine synthetase activity, either by degradation (first negative term) or deactivation (second negative term). The deactivation term again contains a mass action modifier, the scaled ammonia concentration, which generalizes the behavior of the ATase mechanism under the assumption of complete dependence on the ammonia concentration.

The conservation equation for the first nitrogen regulator, NR_I , contains two means of production. The first positive term describes the endergonic assembly reaction of the protein from its amino acid precursors. This term simplifies to a constant maximum transcriptional production rate in the complete absence of regulator, while asymptotically approaching zero as the regulator presence unboundedly increases. The second positive term represents conversion of the phosphorylated form of NR_I back into its unphosphorylated state, as catalyzed by NR_{II} . This is described mathematically through mass action modified again by the scaled ammonia concentration.

The first nitrogen regulator is removed from the cell in two ways. The first negative term accounts for molecular breakdown induced by metabolic degradation. The second negative term accounts for phosphorylation. Its form resembles the dephosphorylation reaction, except that the reactants are now the unphosphorylated forms of both regulators and the modifier is inversely related to the ammonia proportion.

The mass balance equation for the second nitrogen regulator incorporates negatively autoregulated transcription and inherent degradation. The forms of the production and degradation terms resemble those mentioned previously, but with their own specific constants. The transcriptional regulation term allows maximum second regulator production to occur when no inhibitory first regulator is present. Conversely, second regulator production tends to zero as the concentration of the first regulator becomes large.

The rate change equation for the phosphorylated form of NR_I has two conversion terms—one for creation and the other for depletion—and a degradation term. Creation occurs when two regulator molecules successfully interact. The success of this interaction is consistently controlled by the affinity coefficient and the inverse unity-scaled ammonia concentration. It is variably controlled by the product of the independent concentrations of either regulatory gene product. Depletion occurs in a similar fashion, except for the substitution of

a direct unity-scaled ammonia term in place of the inverse modifier. The last term in this equation is the inherent degradation term, which shares the same intrinsic constant of decay as the other two regulator versions.

The negative terms in the ammonia equation stem from two sources of consumption. The first negative term represents the ammonia assimilation reaction catalyzed by glutamine synthetase. The other negative term describes lumped ammonia consumption and removal from the cell; this activity is modeled as a linear process. Lastly, the positive term represents ammonia flux into the cell via any other mechanism. These mechanisms include but are not limited to metabolic production, active transport, and chemical conversion. They are generalized into a single term that accounts for the primary routes of cellular ammonia homeostasis.

Model (1) was converted into non-dimensional form with the following substitutions:

$$\tau = \delta t; x_1 = \frac{N_1}{\kappa_2}; x_2 = \frac{\beta_1 N_2}{v_1}; x_3 = \frac{\beta_2 N_3}{v_2}; y = \frac{\mu G}{\alpha_1}; z = \frac{N_4}{\varepsilon}. \quad (2)$$

These substitutions permit system (1) to take the following form:

$$\begin{aligned} \frac{dy}{d\tau} &= \mu \alpha_2 x_3^2 \left[\frac{\delta \alpha_1 \beta_2^2 (\lambda + \kappa_1 \kappa_2 x_1)}{v_2^2} + x_3^2 \right]^{-1} + y \left[\frac{v_2 + z(v_1 - v_2)}{\delta} - 1 \right], \\ \frac{dx_1}{d\tau} &= \frac{\alpha_2}{\kappa_2 \delta (1 + x_1)} + \left(\frac{v_1 x_2}{\beta_1 \delta} \right) \left[z \left(\frac{\beta_1 v_2 x_3}{\kappa_2 \beta_2} + x_1 \right) \right] - x_1, \\ \frac{dx_2}{d\tau} &= \frac{\alpha_2 \beta_1}{v_1 \delta (1 + x_1)} - x_2, \\ \frac{dx_3}{d\tau} &= \frac{\beta_2 v_1 x_2}{\beta_1 \delta} \left[\frac{\kappa_2 \beta_2 x_1}{v_2} - z \left(\frac{\beta_2 \kappa_2 x_1}{v_2} + x_3 \right) \right] - x_3, \\ \frac{\varepsilon \delta}{\psi} \frac{dz}{d\tau} &= \frac{\phi}{\psi} - z \left(\frac{\phi}{\psi} + \frac{\alpha_1 y}{\psi} + 1 \right). \end{aligned} \quad (3)$$

System (3) can be further simplified with the following parameter groupings:

$$\begin{aligned}
A_1 &= \frac{v_2^2}{\delta\lambda\beta_2^2}; A_2 = \frac{\kappa_1\kappa_2}{\lambda}; \\
B_1 &= \frac{\alpha_2}{\delta\kappa_2}; B_2 = \frac{v_1}{\delta\beta_1}; B_3 = \frac{v_2\beta_1}{\kappa_2\beta_2}; \\
C_1 &= \frac{\beta_1\alpha_2}{\delta v_1}; D_1 = \frac{v_1\beta_2}{\delta\beta_1}; D_2 = \frac{\beta_2\kappa_2}{v_2},
\end{aligned} \tag{4}$$

which produces the following dimensionless model (3):

$$\begin{aligned}
\frac{dy}{d\tau} &= \frac{\mu A_1 x_3^2}{1 + A_2 x_1 + A_1 x_3^2} + y \left[\frac{v_2 + z(v_1 - v_2)}{\delta} - 1 \right], \\
\frac{dx_1}{d\tau} &= \frac{B_1}{1 + x_1} + B_2 x_2 \left[z(B_3 x_3 + x_1) \right] - x_1, \\
\frac{dx_2}{d\tau} &= \frac{C_1}{1 + x_1} - x_2, \\
\frac{dx_3}{d\tau} &= D_1 x_2 \left[D_2 x_1 - z(D_2 x_1 + x_3) \right] - x_3, \\
\frac{\varepsilon\delta}{\psi} \frac{dz}{d\tau} &= \frac{\phi}{\psi} - z \left(\frac{\phi}{\psi} + \frac{\alpha_1 y}{\psi} + 1 \right).
\end{aligned} \tag{5}$$

An underlying assumption of the model is that ATP, NADPH, α -ketoglutarate, and glutamate dehydrogenase are abundant and therefore do not limit nitrogen assimilation. In reality, assimilation is regulated by the ratio of α -ketoglutarate to glutamine, which in this model is translated into the ammonia concentration. A high ratio indicates excess α -ketoglutarate and suggests that the reaction catalyzed by glutamine dehydrogenase has been halted due to low ammonia levels. Conversely, a low ratio means an excess of glutamine and indicates that glutamine synthetase is failing to catalyze its reaction because high

ammonia levels have inhibited enzyme production. Therefore, the model uses ammonia concentration as the direct signaling factor.

Although five equations were needed to describe the entire system, the ammonia concentration can be treated as a constant because it is on a dynamically faster time-scale than the production of glutamine synthetase and the two regulators. The rate change of ammonia becomes zero by assuming the single perturbation is very large based on the appropriate parameter values. The resulting four equation subsystem provides a simpler version of the basis for the entire nitrogen assimilation switch. This approximation contains only the equations for y , x_1 , x_2 , and x_3 ; it treats the ammonia concentration as a constant.

This quasi-steady state assumption is supported by pertinent empirical biochemistry. The production time of the nitrogen assimilation enzymes, including transcription, translation and post-translational modification, is expected to be on the order of hours. Interaction between the *glnL* and *glnG* proteins happens on the order of seconds. The depletion of ammonia through the reaction catalyzed by glutamine synthetase also proceeds at a much faster pace than transcription. The initial ammonia reserve, ammonia in the surrounding media, and ammonia generated from intracellular anabolism are all assumed to have reached equilibrium. The pseudo-steady-state argument also applies to the interactions between PII, ATase, UTase/UR, and the *glnALG* products.

4 Parameterization

The affinity of phosphorylated NR_i for the *glnAp2* promoter, represented by λ , is the strongest enhancer affinity in the *glnALG* operon [11]. This means that transcriptional upregulation presides if equal amounts of the positive and negative regulators are present. Similarly, the NR_i affinity for *Ap1*, represented by κ_1 , is stronger than its affinity for *glnLp*, represented by κ_2 . The ability of other intracellular molecules, such as acetylphosphate, to phosphorylate NR_i is

neglected because the interaction between NR_I and NR_{II} occurs much quicker after ammonia fluctuation [12]. Likewise, phosphorylated NR_I dephosphorylates itself, but at a negligibly slow rate relative to the activity of NR_{II} .

Table 1 A list of all the constants used throughout the progressions of the model.

Parameter	Definition	Units
α_1	Maximum glutamine synthetase transcription rate	$\frac{\text{concentration}}{\text{time}}$
α_2	Maximum regulator transcription rate	$\frac{\text{concentration}}{\text{time}}$
κ_1	Regulator affinity for the glnA promoters	<i>concentration</i>
κ_2	NR_I affinity for the glnLG promoter	<i>concentration</i>
λ	NR_P affinity for the second glnA promoter	<i>concentration</i> ²
δ	Molecular degradation rate	<i>time</i> ⁻¹
β_1	Attraction between NR_P and NR_{II}	<i>time</i> ⁻¹ <i>concentration</i> ⁻¹
β_2	Attraction between NR_I and NR_{II}	<i>time</i> ⁻¹ <i>concentration</i> ⁻¹
v_1	Attraction between glutamine synthetase and PII-stimulated ATase	<i>time</i> ⁻¹
v_2	Attraction between glutamine synthetase and PII-UMP-stimulated ATase	<i>time</i> ⁻¹
μ	Reaction rate for glutamine synthetase-mediated consumption	<i>time</i> ⁻¹
ψ	Ammonia elimination rate	$\frac{\text{concentration}}{\text{time}}$

φ	Ammonia allocation rate	$\frac{\text{concentration}}{\text{time}}$
ε	Maximum intracellular ammonia concentration	<i>concentration</i>

The dimension scaling process completely removed one parameter, ε . Consequently, only one parameter was eliminated from the four-equation subsystem. This action necessitated some term cancellation and reduced the complexity of the resulting steady states.

The maximum transcription rates, represented by α_1 and α_2 , were expected to fall within a range of 0.5 to 2.4 molecules per cell per minute or 30 to 144 molecules per hour [13]. The regulator affinities for the promoters, represented by κ_1 , and κ_2 were taken to be in the range of 0.027 to 1.4 micromoles per liter [14]. The enzyme degradation rate, represented by δ , was calculated from the supposed 3 hour half life and resulted in 0.23 per hour [15]. The third regulator affinity, represented by λ , was assumed to resemble the square of either of the previous affinities, which computed to a range of 0.00073 to 1.96 micromoles² per liter². The intrinsic phosphorylation and dephosphorylation rates between the regulators represented by β_1 and β_2 , were estimated to follow the ratio of the turnover number to the Michaelis constant of bacterial phosphokinase, which carried a value of 0.102 per second per millimole per liter and converted to 0.37 per hour per micromole per liter [16]. The adenylyl deactivation and activation of glutamine synthetase, respectively represented by ν_1 and ν_2 , was suspected to occur at an intrinsic rate of 0.26 per hour [17]. Moreover, the specific activity of glutamine synthetase, represented by μ , was predicted to be 0.048 micromoles per minute per milligram, which converted to 0.002 per hour with a conjectured molecular weight of 6.8×10^5 daltons [18]. The elimination of ammonia, represented by ψ , via conversion to carbamoyl phosphate was taken to be on the order of 2.8 micromoles per liter per minute or 0.17 millimoles per liter per hour [19]. The allocation rate, represented by φ , was

used in relation to the ammonia uptake seen in other bacteria types, which was on the order of 0.07 micromoles per milligram of source [20]. The maximum intracellular ammonia concentration, represented by ε , was predicted to be about 17 millimoles per liter [21].

5 Results

Steady state characterization was useless due to the complexity of the model (5). For example, the Maple output expressing one of the equilibrium in terms of the parameters extended over at least ten screens. Therefore, no further symbolic steady state analysis was attempted.

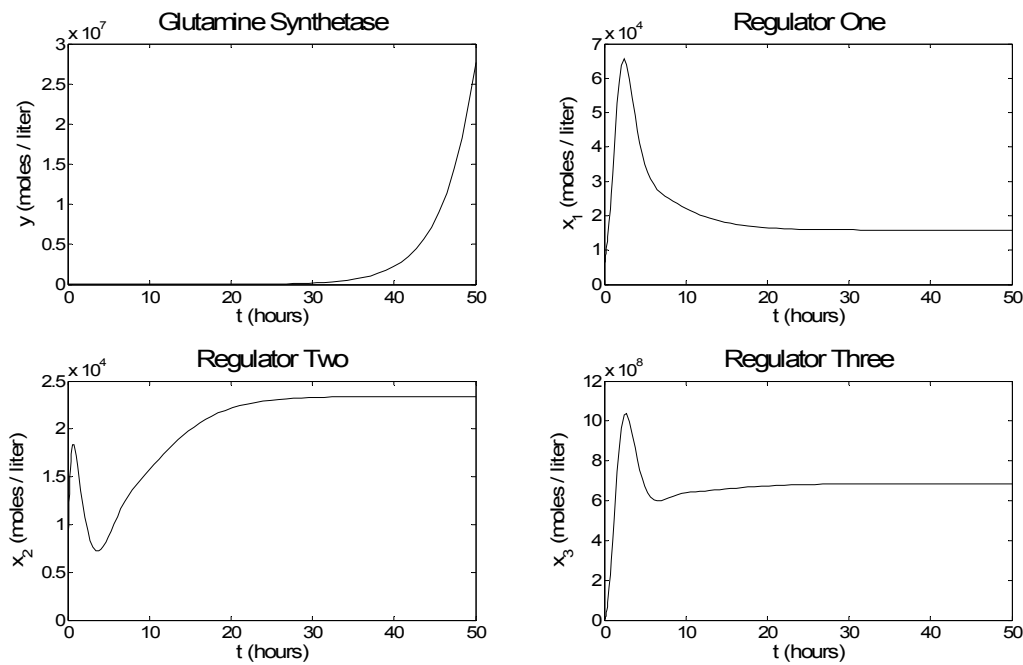


Figure 2 Time dependent concentrations of the various *glnALG* products in the quasi steady-state model. The parameters were set to the following values: $\alpha_1 = 50.0$, $\alpha_2 = 50.0$, $\beta_1 = 0.370 \times 10^6$, $\beta_2 = 0.370 \times 10^6$, $\delta = 0.200$, $\varepsilon = 0.017$, $\kappa_1 = 1.00 \times 10^{-6}$, $\kappa_2 = 1.00 \times 10^{-6}$, $\lambda = 0.100 \times 10^{-6}$, $\mu = 0.005$, $\nu_1 = 0.250$, $\nu_2 = 0.250$, $\varphi = 0.070 \times 10^{-3}$, and $\psi = 0.170 \times 10^{-3}$. The initial conditions were set to the following values: $y_0 = 1.00 \times 10^2$, $x_1 = 0.00$, $x_2 = 10.0$, and $x_3 = 10.0$.

Instead, iterations with different parameter and initial condition sets were used to explore this intricate model. Figure 2 shows the time series for the model that was assumed to have a quasi steady-state ammonia level. The three regulatory enzymes appeared to reach a steady state, which for this specific case was visually extrapolated to be $\sigma_{\text{QSSA}}(100, 0, 10, 10) = (\infty, 1.5 \times 10^4, 2.5 \times 10^4, 7 \times 10^8)$. Figure 3 shows the time series for the full five equation model, which included a variable ammonia concentration. The pseudo fixed point of the regulatory enzymes and nitrogen source for this specific case was visually extrapolated to be $\sigma_{\text{FULL}}(100, 0, 10, 10, 0.1 \times 10^6) = (\infty, 1.5 \times 10^4, 2.5 \times 10^4, 7 \times 10^8, 0)$.

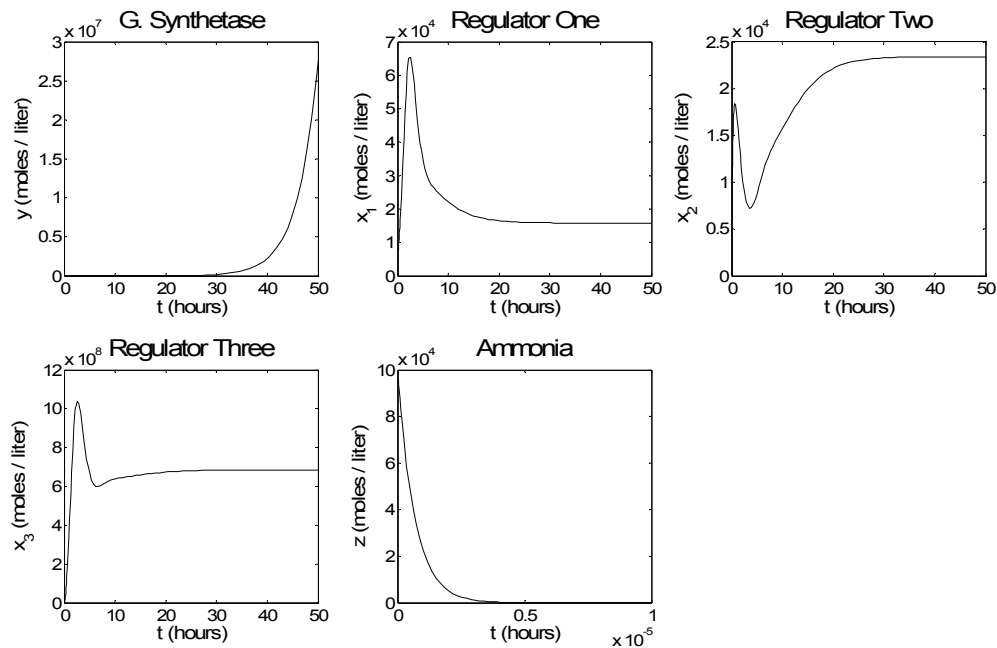


Figure 3 Time dependent concentration of the *glnALG* products as well as the ammonia concentration. This model was solved without the quasi steady-state assumption. The parameters were set to the following values: $\alpha_1 = 50.0$, $\alpha_2 = 50.0$, $\beta_1 = 0.370 \times 10^6$, $\beta_2 = 0.370 \times 10^6$, $\delta = 0.200$, $\varepsilon = 0.017$, $\kappa_1 = 1.00 \times 10^6$, $\kappa_2 = 1.00 \times 10^6$, $\lambda = 0.100 \times 10^6$, $\mu = 0.005$, $v_1 = 0.250$, $v_2 = 0.250$, $\varphi = 0.070 \times 10^{-3}$, and $\psi = 0.170 \times 10^{-3}$. The initial conditions were set to the following values: $y_0 = 1.00 \times 10^2$, $x_1 = 0.00$, $x_2 = 10.0$, $x_3 = 10.0$, and $z_0 = 0.100 \times 10^6$.

Furthermore, an iterative look at parameter sensitivity was facilitated by graphing the effects of parameter adjustment on interrelationships among a

subset of the dependent variables. Figure 4 shows three discrete changes in regulator enzyme dynamics corresponding with three different combinations of maximum transcription rates. Similarly, figure 5 shows three discrete changes in regulator enzyme dynamics corresponding with three different combinations of maximum phosphorylation rates.

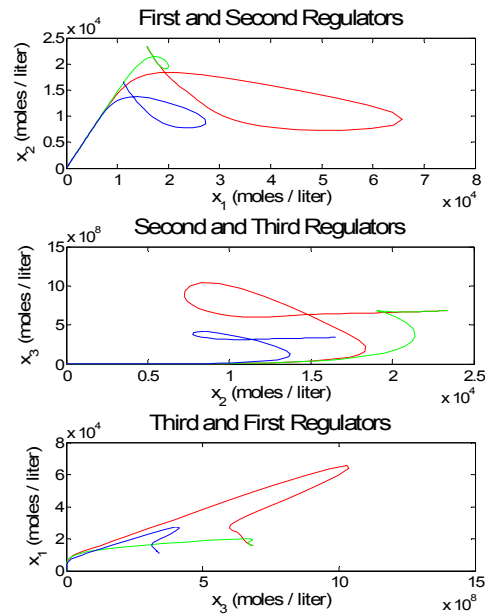


Figure 4 Several solution contours of the various regulator products for the quasi-steady state model. The red lines correspond to $a_1 = 50.0$ and $a_2 = 50.0$. The green lines correspond to $a_1 = 5.00 \times 10^2$ and $a_2 = 50.0$. The blue lines correspond to $a_1 = 50.0$ and $a_2 = 25.0$. The rest of the parameters were set to the following values for all of the iterations: $\beta_1 = 0.370 \times 10^6$, $\beta_2 = 0.370 \times 10^6$, $\delta = 0.200$, $\varepsilon = 0.017$, $\kappa_1 = 1.00 \times 10^{-6}$, $\kappa_2 = 1.00 \times 10^{-6}$, $\lambda = 0.100 \times 10^{-6}$, $\mu = 0.005$, $v_1 = 0.250$, $v_2 = 0.250$, $\varphi = 0.070 \times 10^{-3}$, and $\psi = 0.170 \times 10^{-3}$. The initial conditions were set to the following values: $y_0 = 100$, $x_1 = 0$, $x_2 = 10$, and $x_3 = 10$.

Figure 6 shows three slices of the feedback enzyme dynamics according to three different pairs of glutamine synthetase maximum activation rates.

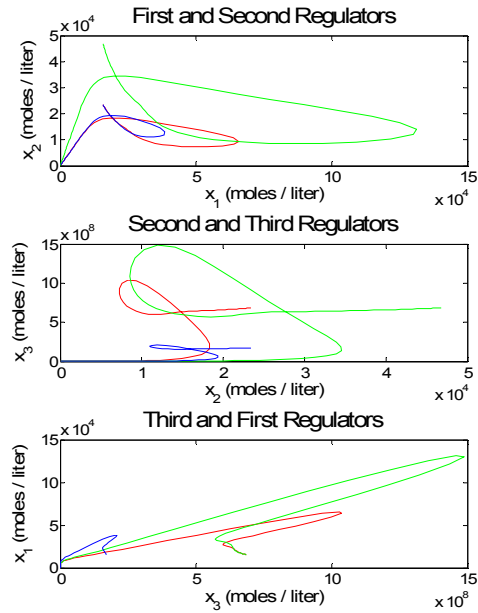


Figure 5 Several solution contours of the various regulator products for the quasi-steady state model. The red lines correspond to $\beta_1 = 0.370 \times 10^6$ and $\beta_2 = 0.370 \times 10^6$. The green lines correspond to $\beta_1 = 0.740 \times 10^6$ and $\beta_2 = 0.370 \times 10^6$. The blue lines correspond to $\beta_1 = 0.370 \times 10^6$ and $\beta_2 = 0.185 \times 10^6$. The rest of the parameters were set to the following values for all of the iterations: $\alpha_1 = 50.0$, $\alpha_2 = 50.0$, $\delta = 0.200$, $\varepsilon = 0.017$, $\kappa_1 = 1.00 \times 10^{-6}$, $\kappa_2 = 1.00 \times 10^{-6}$, $\lambda = 0.100 \times 10^{-6}$, $\mu = 0.005$, $v_1 = 0.250$, $v_2 = 0.250$, $\varphi = 0.070 \times 10^{-3}$, and $\psi = 0.170 \times 10^{-3}$. The initial conditions were set to the following values: $y_0 = 100$, $x_1 = 0$, $x_2 = 10$, and $x_3 = 10$.

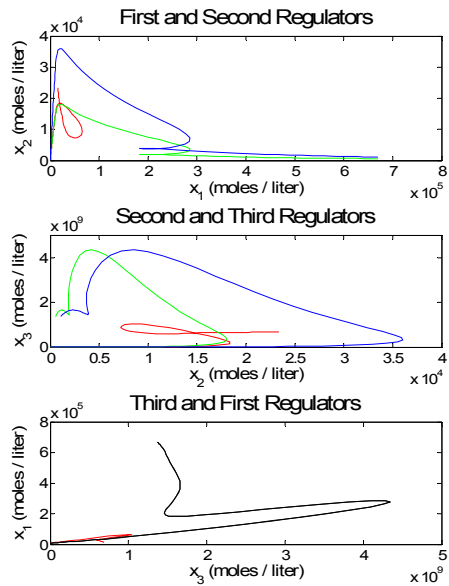


Figure 6 Several solution contours of the various regulator products for the quasi-steady state model. The red lines correspond to $v_1 = 0.250$ and $v_2 = 0.250$. The green lines correspond to $v_1 = 0.250$ and $v_2 = 0.125$. The blue lines correspond to $v_1 = 0.125$ and $v_2 = 0.125$. The black line shows where both the green and blue lines would have appeared

undistinguishable from one another. The rest of the parameters were set to the following values for all of the iterations: $\alpha_1 = 50.0$, $\alpha_2 = 50.0$, $\beta_1 = 0.370 \times 10^6$, $\beta_2 = 0.370 \times 10^6$, $\delta = 0.200$, $\varepsilon = 0.017$, $\kappa_1 = 1.00 \times 10^{-6}$, $\kappa_2 = 1.00 \times 10^{-6}$, $\lambda = 0.100 \times 10^{-6}$, $\mu = 0.005$, $\varphi = 0.070 \times 10^{-3}$, and $\psi = 0.170 \times 10^{-3}$. The initial conditions were set to the following values: $y_0 = 100$, $x_1 = 0$, $x_2 = 10$, and $x_3 = 10$.

6 Discussion and Conclusions

The results of the preliminary steady state analysis classified both the four and five equation models unsusceptible to symbolic steady state interpretation. This difficulty was circumvented with visual steady state approximations. Steady state inspection of figure 2 suggested the quasi steady state assumption for ammonia was valid.

Interestingly, the prediction that the constant ammonia concentration would remain at the initial ammonia concentration was refuted. Ironically, the ammonia concentration reached a value negligibly close to zero according to the plot of ammonia versus time in figure 3.

It was expected that the difference between v_1 and v_2 would have a more profound effect on the dynamics than the absolute magnitudes, but the numerical results suggest the exact opposite. It appears that v_2 is more sensitive than v_1 because changes in v_1 only induce proportional vertical or horizontal shifts, whereas changes in v_2 tend to induce visually detectable shape adjustments. The graphs in figure 6 show that the shape of the plots is affected more by the absolute value of v_2 than by the difference between v_1 and v_2 .

References

- [1] Savageau, M. A. (1974). Comparison of classical and autogenous systems of regulation in inducible operons. *Nature*, **252**, 546-9.
- [2] Rosenfeld, N., Elowitz, M. B., and Alon, U. (2002). Negative autoregulation speeds the response times of transcription networks. *Journal of Molecular Biology*, **323**, 785-93.

- [3] Atkinson, M.R., Savageau, M.A., Myers, J.T., and Ninfa, A.J. (2003). Development of genetic circuitry exhibiting toggle switch or oscillatory behavior in *Escherichia coli*. *Cell*, **113**, 597-607.
- [4] Smolen, P., D.A. Baxter, and J.H. Byrne (1998). Frequency selectivity, multistability, and oscillations emerge from models of genetic regulatory Systems. *American Journal of Physiology*, **274**, C531–42.
- [5] Magasanik, B. (1996). Regulation of nitrogen assimilation. In: *Regulation of Gene Expression in Escherichia coli*, ed. E.C.C. Lin and A. Simon, pp. 281-90. Austin: R.G. Landes Company.
- [6] Brenchley, J.E., M.J. Prival, and B. Magasanik (1973). Regulation of the synthesis of enzymes responsible for glutamate formation in *Klebsiella aerogenes*. *Journal of Biological Chemistry*, **248**, 6122-28.
- [7] Tyler, B. (1978). Regulation of the assimilation of nitrogen compounds. *Annual Reviews in Biochemistry*, **47**, 1127-62.
- [8] Magasanik, B. (1988). Reversible phosphorylation of an enhancer binding protein regulates the transcription of bacterial nitrogen utilization genes. *TIBS*, **13**, 475-79.
- [9] Ninfa, A.J., and B. Magasanik (1986). Covalent modification of the *glnG* product, NR_I, by the *glnL* product, NR_{II}, regulates the transcription of the *glnALG* operon in *Escherichia coli*. *Proceedings of the National Academy of Science in the United States of America*, **83**, 5909-13.
- [10] Snyder, Larry and Wendy Champness (1997). *Molecular Genetics of Bacteria*. Washington, D.C.: ASM Press.
- [11] Weiss, V., F. Claverie-Martin, and B. Magasanik (1992). Phosphorylation of nitrogen regulator I of *Escherichia coli* induces strong cooperative binding to DNA essential for activation of transcription. *Proceedings of the National Academy of Science in the United States of America*, **89**, 5088-92.

- [12] Feng, J., M.R. Atkinson, and W. McCleary (1992). Role of phosphorylated metabolic intermediates in the regulation of glutamine synthetase synthesis in *Escherichia coli*. *Journal of Bacteriology*, **174**, 6061-70.
- [13] Brock, M. L. and D. J. Shapiro (1983). Estrogen regulates the absolute rate of transcription of the *Xenopus laevis* vitellogenin genes. *Journal of Biological Chemistry*, **256**, 9, 5449-55.
- [14] Vazquez, M. F., E. Flores, and A. Herrero (2002). Analysis of binding sites for the nitrogen-control transcription factor NtcA in the promoters of *Synechococcus* nitrogen-regulated genes. *Biochemistry and Biophysics*, **1578**, 1-3, 95-8.
- [15] Spooner, R. A., *et al* (2003). A novel vascular endothelial growth factor-directed therapy that selectively activates cytotoxic prodrugs. *British Journal of Cancer*, **88**, 10, 1622-30.
- [16] Bertrand, T., *et al* (2002). Sugar specificity of bacterial CMP kinases as revealed by crystal structures and mutagenesis of *Escherichia coli* enzyme. *Journal of Molecular Biology*, **315**, 1099-110.
- [17] Jouanneau, Y., S. Lebecque, and P. M. Vignais (1984). Ammonia and light effect on nitrogenase activity in nitrogen-limited continuous cultures of *Rhodospseudomonas capsulate* role of glutamine synthetase. *Archives of Microbiology*, **139**, 4, 326-31.
- [18] Woolfolk, C. A., B. Shapiro, and E. R. Stadtman (1966). Regulation of glutamine synthetase: purification and properties of glutamine synthetase from *Escherichia Coli*. *Archives of Biochemistry and Biophysics*, **116**, 177-92.
- [19] Fahien, L. A. and P. P. Cohen (1964). A kinetic study of carbamyl phosphate synthetase. *Journal of Biological Chemistry*, **239**, 1925-34.
- [20] Poole, P. S., M. J. Dilworth, and A. R. Glenn (1987). Ammonia is the preferred nitrogen source in several *Rhizobia*. *Journal of General Microbiology*, **133**, 7, 1707-12.

- [21] Cabral, J. P. (1994). Comparison of methods to assay ammonia in bacterial suspensions. *Journal of Microbiological Methods*, **19**, 3, 207-13.